EXPERIMENTAL INVESTIGATION OF FLOW PARAMETERS IN A MILD CURVED S-SHAPED DIFFUSING DUCT

Amar Nath Mullick* and Bireswar Majumder**

Abstract

The paper presents a detailed study of the performance of fully developed subsonic turbulent flow in a circular cross-section S-shaped centerline-diffusing duct. A precalibrated 5-hole pressure probe was used for the measurements. The diffuser cross-section was expanded to 2.25 area ratio (A_r) at the exit. The duct was fabricated by joining two 22.5° bends of curvature ratio (β_t) 11.46 in reverse direction with a centerline offset of 0.2 of the axial length of the diffuser. The test was carried out with inlet R_e=8.4x10^5, calculated based on diffuser inlet diameter. The experimental results indicated the generation of secondary flow in the form of a pair of counter rotating vortices in the first half, which changes its senses of rotation in the second half. The overall static pressure recovery of the diffuser was 40%.

Nomenclature

A_r = area ratio
cc = concave or inside wall
C_{pitch} = pitch coefficient
C_{PR} = coefficient of pressure recovery
C_{static} = static pressure coefficient
C_{total} = total pressure recovery
cv = convex or outside wall
C_{yaw} = yaw coefficient
D = diameter
D_h = hydraulic diameter
D_n = Dean number
N = length of the diffuser centerline
O_f = offset of centerline
P = pressure
P_s = static pressure
P_{sw} = wall static pressure
P_T = total pressure
R_e = Reynolds number
U = velocity component in X-direction
U_{av} = mass averaged mean velocity
α = pitch angle
β = yaw angle
ξ = coefficient of pressure loss
$\Delta\beta$ = angle of turn of the centerline
β_t = curvature ratio (radius of curvature/hydraulic diameter)
θ = half of the divergent angle

Subscripts

av = average
i = inlet
e = exit
B = bottom
C = center
L = left
R = right
T = top

Superscript

- = average of any flow properties

Introduction

S-shaped diffusing ducts are commonly used as aircraft intake ducts to re-direct the flow as well as to achieve pressure recovery with the requirement of minimum distortion of the velocity distribution at the compressor face. The flow in these ducts is complicated due to the inflexion in the curvature along the direction of flow.

The performance as well as the flow characteristics of this type of diffuser is strongly dependent on various geometrical and dynamic parameters like, area ratio (A_r), divergence angle (2θ), angle of turn of the centerline ($\Delta\beta$), slenderness ratio (N/D_i), inlet Reynolds number (R_e), inlet Mach number (M) and inlet boundary layer blockage

* Assistant Professor, Department of Mechanical Engineering, FIEM, Kolkata-700 150, India
** Reader, Department of Power Engineering, Jadavpur University, Kolkata-700 098, Email : b_maj3255@yahoo.com
Manuscript received on 16 May 2005; Paper reviewed, revised and accepted on 22 Nov 2005

factor (B_t) etc. These parameters are defined in Fig. 1 at the end of the text section. Therefore, to design an efficient S-shaped diffuser, even with the available different flow prediction code, a detailed experimentally obtained high quality flow data is required.

Studies on constant area S-duct with circular cross-section have been reported in literature [1], [2], [3]. These studies showed the development of a pair of counter rotating vortices within the duct. Development of secondary motion with higher intensity of laminar flow conditions due to the thicker inlet boundary layer at the inlet within an S-shaped duct of mild curvature has been reported by Taylor et al. [4]. They observed that the magnitude of radial velocity reduces towards the exit of the duct. Sometime around eighties of last centuary, researchers initiated work in S-shaped ducts with varying cross-sectional area, based on the acquired knowledge from the constant area ducts. Rojas et al. [5] investigated the flow characteristics in a circular cross-section S-shaped diffuser of A_r = 1.5 and $\Delta\beta$ was fixed at 22.5º/22.5º. Development of secondary motions similar to those in constant area ducts [4] has been observed. Guo and Seddon [6] studied the effect of swirl and offset on two planes in an S-shaped diffusing duct. They showed that the vertical offset increases the magnitude of self-generated swirl, whereas the horizontal offset reduces its magnitude. Detailed 3-D turbulent flow characteristics in a circular cross-section S-shaped diffuser have been carried out by Whitelaw and Yu [7] with O_f = 0.3 and $\Delta\beta$ = 22.5º/22.5º. They used LDA and refractive index matching techniques with two different boundary layer thicknesses. The studies revealed that the larger size of contra rotating vortices exists at the diffuser exit for thinner boundary layer as compared to thicker boundary layer. As a result, the mean exit flow distribution consisted of a larger pair of counter rotating vortices, which were occupying almost half of the cross-sectional area. Shimizu et al. [8] reported studies on V-shaped and twisted S-shaped (snake coil shape) diffusers of circular cross-section for various area ratios. They observed better performance of the twisted S-shaped diffuser for distorted inlet velocity profile. Flow development within an S-shaped diffuser of rectangular section of A_r = 2.0 of strong centerline curvature of $\Delta\beta$ = 90º/90º was studied by Majumder et al. [9]. It has been observed that the generation of secondary motion within the diffuser is mainly due to the imbalance of centrifugal force and radial pressure gradient. They also observed uniform flow at the exit. However, the pressure recovery of the diffuser is low in comparison to a straight diffuser. Similar phenomena were observed by Sullery et al. [10]. They observed that the growth of inner surface boundary layer has a major effect on the losses in case of a curved diffuser. The flow characteristics within an annular S-shaped diffusing duct were studied by Sonoda [11]. It has been observed that the total pressure loss near the hub is largely due to instability of flow as compared with that near the casing and total pressure loss near the hub is more compared with the case of straight annular passage. In all those experiments, the studies have been made to observe the flow characteristics caused by the effect of the centerline curvature. The present study has been undertaken to isolate and establish the effect of wall curvature in an S-shaped diffusing duct. The geometry of the diffusing duct was such that there was little likelihood of flow detachment, because the displacement of the centerline was small and the curvature of the centerline was mild. In this investigation measurements for the flow in a 22.5º/22.5º diffusing duct have been presented. The diffusion is accomplished by linearly increasing cross-sectional area and the centerline of the diffuser was chosen as circular.

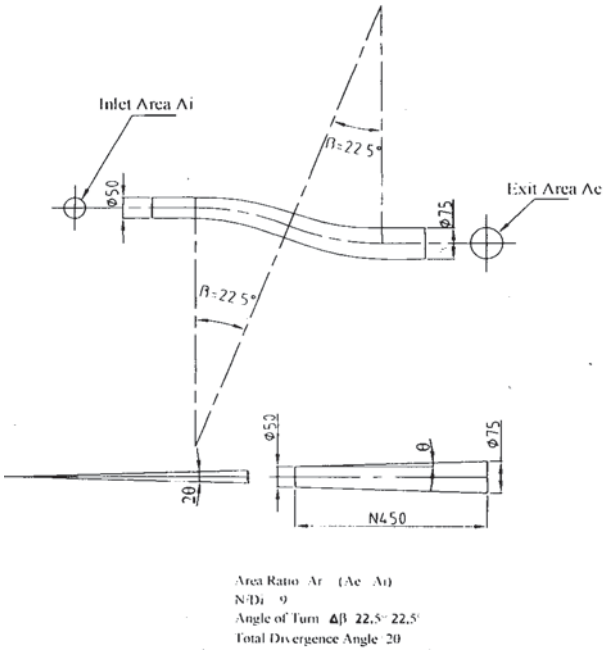

Fig. 1 Definition of geometrical parameters

Flow Configuration, Instrumentation and Experimental Procedure

A schematic diagram of the experimental set-up is shown in Fig.2. The main component of the experimental set-up comprises an air supply unit, which is capable' of delivering 0.6m^3/s of air at a pressure of 0.1m of water

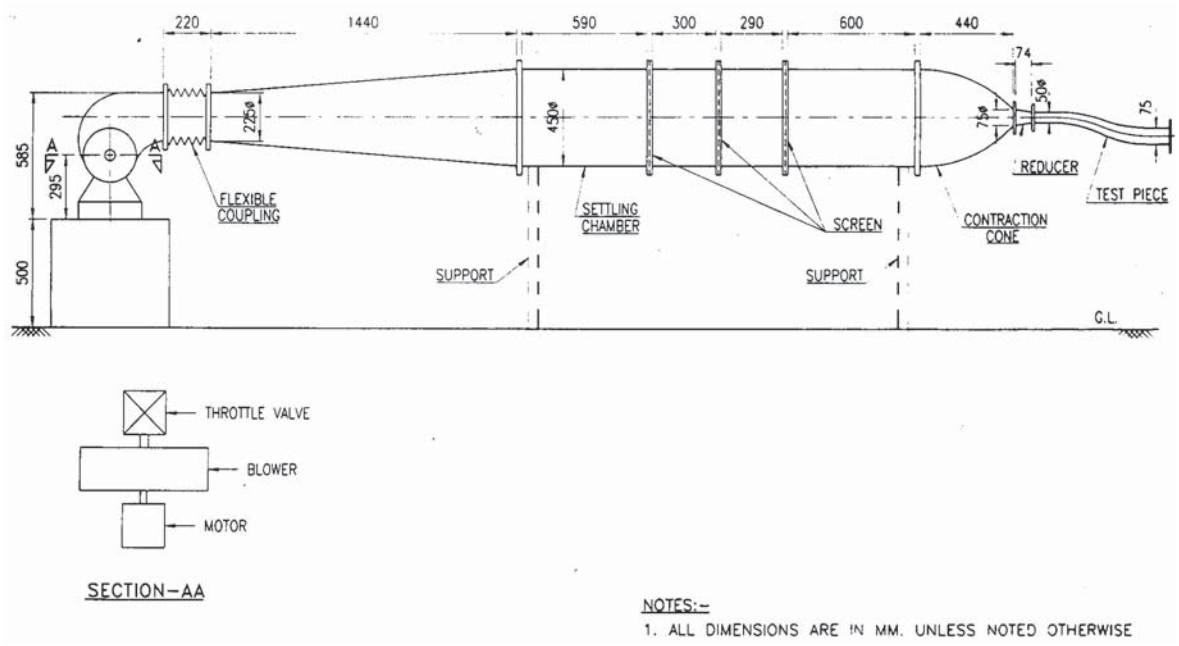

Fig. 2 Schematic layout of the experimental setup

column, a conical diffuser and a settling chamber fitted with fine mesh nylon screens for straightening the flow. The air from settling chamber enters into the test diffuser preceded by a contraction cone and a small entry duct.

The geometry of the test diffuser is shown in Fig.3. The diffuser was designed as suggested by Fox and Kline [12] and based on linear area ratio from inlet to exit distributed normal to the centerline. The test diffuser was designed based on A_r=2.25 with O_f = 0.2N and of circular cross-section. To develop the test diffuser geometry, a straight diffuser of D_i = 50mm with N/D_i = 9.0 and A_r = 2.25 was drawn. The first half of the centerline of the straight diffuser was given a turn for 22.5º with $D_n = 1.76 \times 10^5$.

The other half was turned through 22.5º in the reverse direction with the same radius of curvature. It results to an inflexion point on the curvature and produces the S-shaped of the centerline. The total shape of the test diffuser was made by joining all the points obtained on both sides of the circular centerline on the basis of linearly increase in area. The test diffuser was constructed from fiberglass reinforcement plastic and the diffusing bend was preceded and followed by straight constant area sections having a length of twice the inlet diameter. The purpose of providing constant area duct at exit is to maintain the diffuser performance undisturbed by reducing the atmospheric effect at the exit opening. The inlet section was chosen at one inlet diameter upstream of the diffuser in the constant area duct. Measurements of different flow characteristics like axial and radial velocity, static and total pressure were made at six sections inside the diffuser along with the inlet section. The measuring sections were chosen at all the sections at 0º, 45º, 270º and 315º from the vertical axis of the diffuser. The detailed geometry of the test diffuser along with the measuring stations and co-ordinate system is also shown in Fig.3.

A pre-calibrated 5-hole probe using null technique and controlled by a microprocessor based dual step motorized traversing equipment was used to measure the flow parameters. The pressure on all the 5-holes of the probe was recorded on a multi-tube manometer of variable inclination. The rotation of the stepper shaft was controlled by a ALS-08-PC card installed in the port of the computer with a interfacing of RS-232 modem. The shaft of the stepper motor was coupled to a 300mm long lead screw capable of producing a torque of 0.2950Nm and having a least count of rotational movement 0.9º. The stem of the five holes was connected to the lead screw by an arm.

The calibration of 5-hole probe in terms of various coefficients was determined at different pitch angles (Fig.4). Yaw sensing pressure ports were approximately balanced (within ±5º). The probe coefficients are deter-

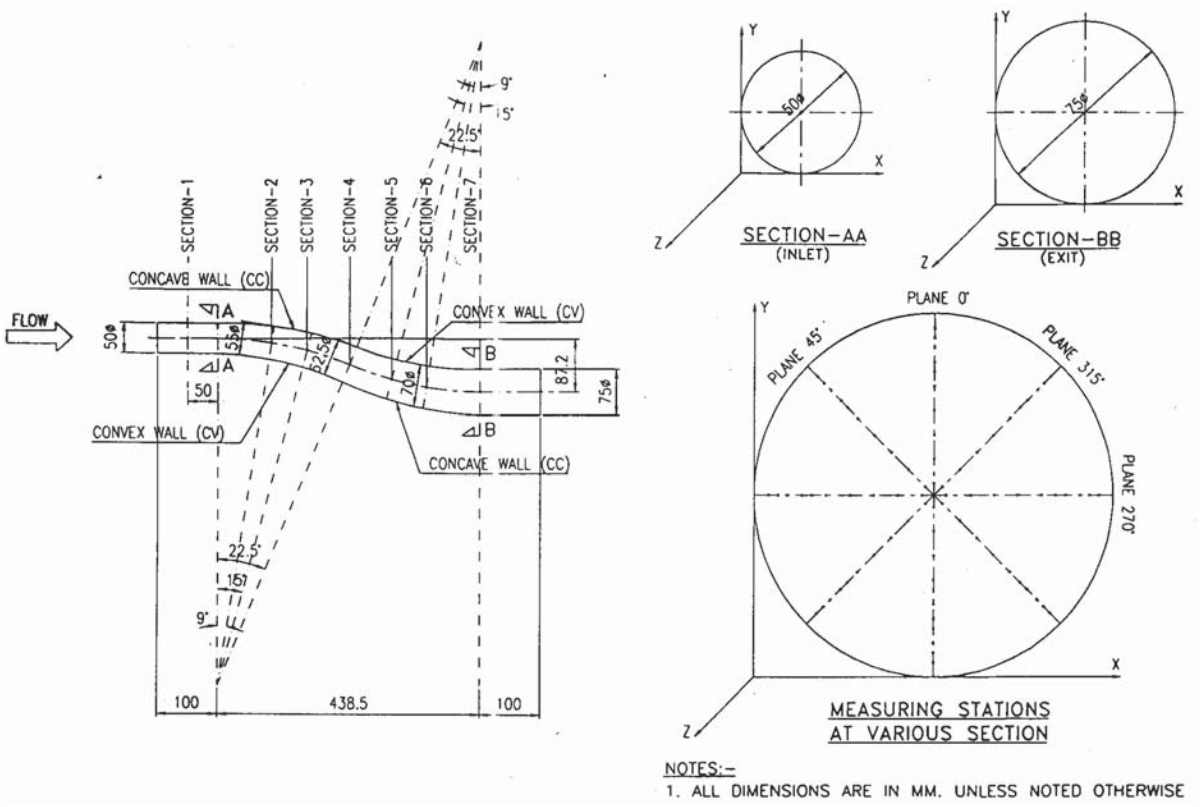

Fig. 3 Dimensions of the test diffuser and defination of co-ordinates

mined as a function of pitch with allowance made for the possibility of a small correction due to slight yaw. At each pitch angle during the time of calibration the probe was yawed approximately ±5° relative to its null position to determine the effect of the small yaw misalignment.

The calibration was done in terms of the following coefficients:

$$C_{pitch} = \frac{P_B - P_T}{P_C - \bar{p}}$$

$$C_{yaw} = \frac{P_R - P_L}{P_C - \bar{p}}$$

$$C_{total} = \frac{P_C - P_T}{P_C - \bar{p}}$$

$$C_{static} = \frac{\bar{p} - P_S}{P_C - \bar{p}}$$

where $\bar{p}$ is the average of the pressure sensed by the two side tubes, i.e.,

$$\bar{p} = \frac{1}{2}(P_L + P_R)$$

Polynomial least square curve fitting as well as spline interpolation has been tried in the present investigation to determine the variation of these coefficients with pitch and yaw plane. However, the polynomial least square curve fitting has been used as it reduces the complexity of computation of the velocity vectors.

From the calibration curve C_{total} and C_{static} were determined and subsequently the mean velocity at each measuring point was calculated by using the formulas:

$$U = \sqrt{\left[\frac{2}{\rho}\left\{(P_c - \bar{p})\,(C_{static} - C_{total} + 1)\right\}\right]}$$

and resolving the velocity vector into its components :

$$U_x = U\cos\alpha\,\cos(\theta + \beta)$$

$$U_y = -\,U\sin\alpha$$

$$U_z = U\cos\alpha\,\sin(\theta + \beta)$$

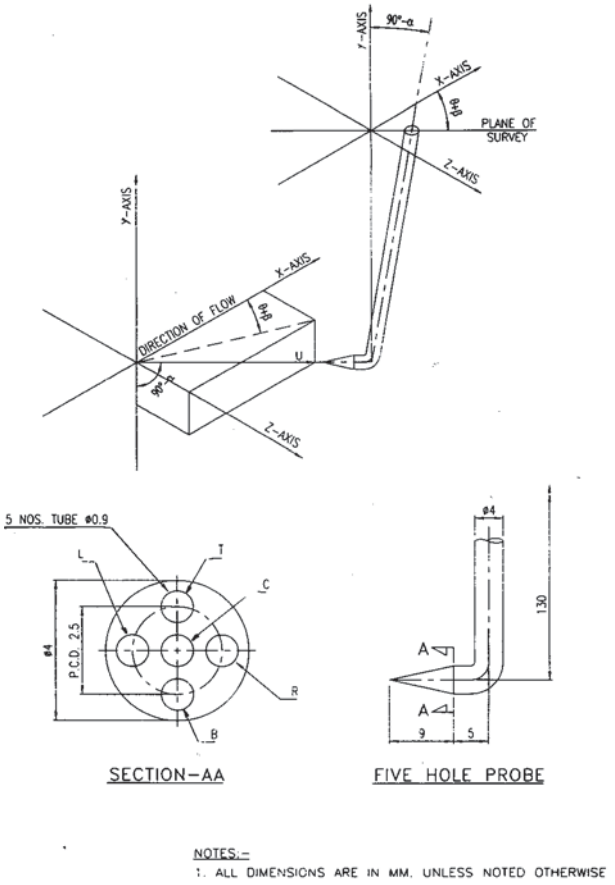

Fig. 4 Pitch angle and yaw angle definition

The method of calibration was done based on the method described by McMillan [13]. The procedure of calibration and measurements by the probe has been discussed in details by Mullick [14].

The coefficient of static pressure recovery and coefficient of total pressure loss have been evaluated from the mass averaged values. The contours have been drawn with the help of SURFER Software.

Uncertainty analysis has been carried out for different measured quantities according to Kline [15]. The uncertainty for the mean velocity, static, dynamic and total pressures are given in Table-1. Besides, while taking the measurements with 5-hole probe the sum of the squares of the residuals is calculated based on the difference of the value predicted by the polynomial least square fitted curve and measured value at all measured points. This sum of the squares of the residuals is tabulated in Table-2. Similar methods are also applied for the calibration coefficients.

Table-1

Quantity	Estimated Uncertainty	
	Lower Flow Rate (U < 10.0 m/s)	Higher Flow Rate (U > 10.0 m/s)
Mean Velocity	± 5.0%	± 1.0%
Pressure (Static and Total)	± 2.0%	± 0.2%
Dynamic Pressure	± 2.0%	± 0.2%
Flow Angle	± 0.5%	± 0.5%

Table-2

Type of Plot	Sum of Square of Residuals
P_C vs . α ($\beta = 0^o$)	0.1460
P_C vs . β ($\alpha = 0^o$)	0.8050
P_B vs . α ($\beta = 0^o$)	2.3960
P_T vs . α ($\beta = 0^o$)	0.6890
P_L vs . β ($\alpha = 0^o$)	1.0670
P_R vs . β ($\alpha = 0^o$)	0.4100
C_{pitch} vs . α ($\beta = 0^o$)	0.0380
C_{yaw} vs . β ($\alpha = 0^o$)	0.0620
C_{static} vs . α ($\beta = 0^o$)	0.0021
C_{total} vs . α ($\beta = 0^o$)	0.0160

Results and Discussions

Flow characteristics have been evaluated by measuring mean velocity, radial components of mean velocity, total pressure, static pressure, dynamic pressure and wall static pressure. Measured flow quantities except wall pressure are represented in contour forms. Flow characteristics like velocities and pressures were normalized with the inlet mass averaged velocity and dynamic pressure respectively.

Profiles of normalized stream wise mean velocity (U/U_{avi}) at seven sections measured at four angles along 0^o, 45^o, 270^o and 315^o in the meridional plane of the diffuser length are presented in Fig.5. From Fig.5(a) it can be observed that the flow is uniform at all the sections.

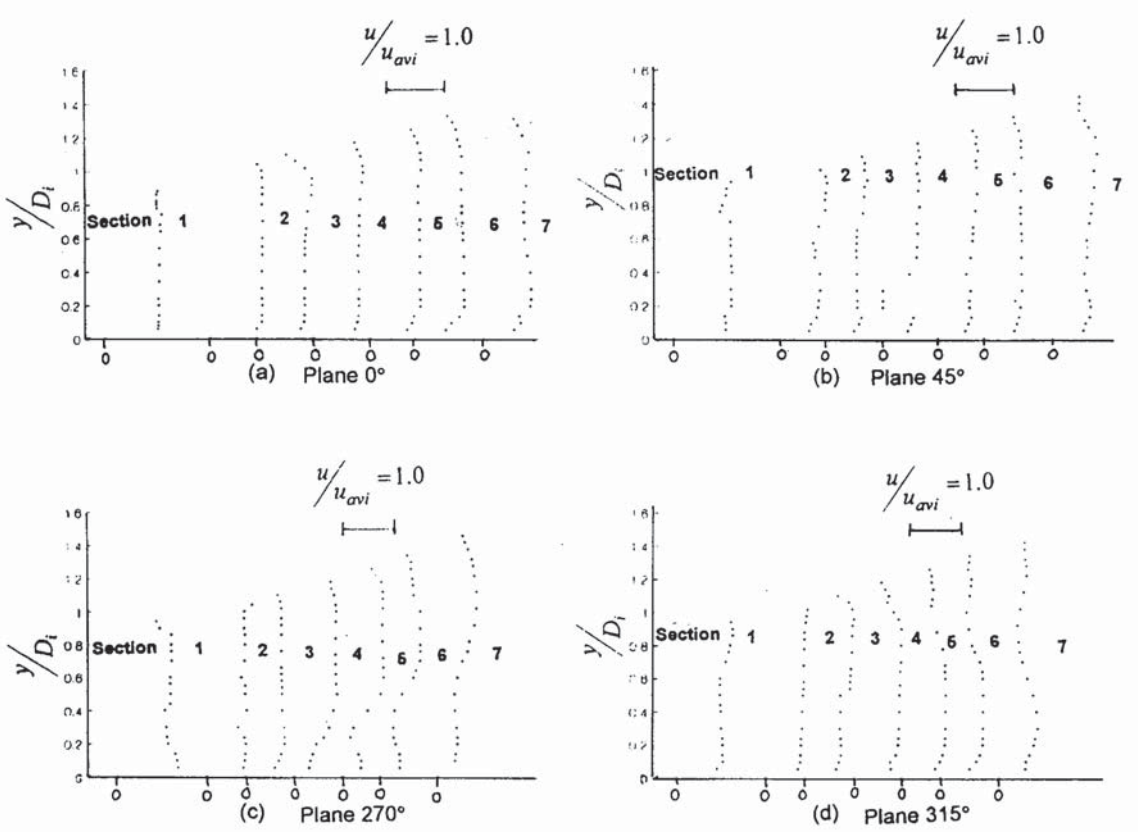

Fig. 5 Mean velociety profile at different measuring plane

From Fig.5(c) it can be observed that the high velocity core moves from outside (cv) to inside (cc) wall and it indicates the change of rotation of the secondary motion as the gradient of velocity profile has changed after section 4. However, continuous deceleration and loss of uniformity has been observed from the figures which is mainly due to the development of secondary flow, a common feature observed for the flow through curved ducts [1], [2], [3]. No flow separation observed throughout the entire length of the diffuser. To have better understanding of the flow development in the test diffuser contours of mean velocity, contours of radial velocity have been drawn and are shown in Fig. 6 and 7 respectively. Fig.6(a) indicates that the flow is asymmetric close to the convex wall at inlet section of the diffuser. The high velocity fluid is accumulated at the bottom right side of the vertical symmetry plane at inlet, which is attributed to the downstream curvature effect. The high velocity fluids divides the entire cross-sectional area into two parts which indicates the generation of counter rotating vortical motions in the form of secondary motion inside the diffuser, as noticed from Fig. 6(b) to 6(g). In the first half of the bend the high velocity core moves in clockwise direction from outside wall (cc) to inside wall (cv). At the inflexion section the acceleration of flow shifted from inside wall (cv) to outside wall (cc), which is mainly due to the combined effect of centrifugal force and change of flow direction in the downstream section. The Fig.6(e) and 6(f) depicts that low velocity fluid occupies more or less one quarter of the hydraulic diameter of the diffuser at the bottom face. The low velocities at these sections near the top and bottom face also clearly divides the bulk flow into two regions, one part towards the outside wall (cc) of the upper half and other part towards the inside wall (cv) of the lower half. Further downstream, Fig.6(g) it can be observed that the secondary vortical motion, generated at the first half of the bend also persists in the second bend, but the sense of rotation of the pair of vortices is opposite to that of the first half with respect to the curved wall of the diffuser. Here sense of rotation means that the rotation of the secondary motion with respect to the solid boundary of the diffuser wall. The overall diffusion of the flow as well as large region of non-uniform distribution of contour near the bottom face is observed at this section.

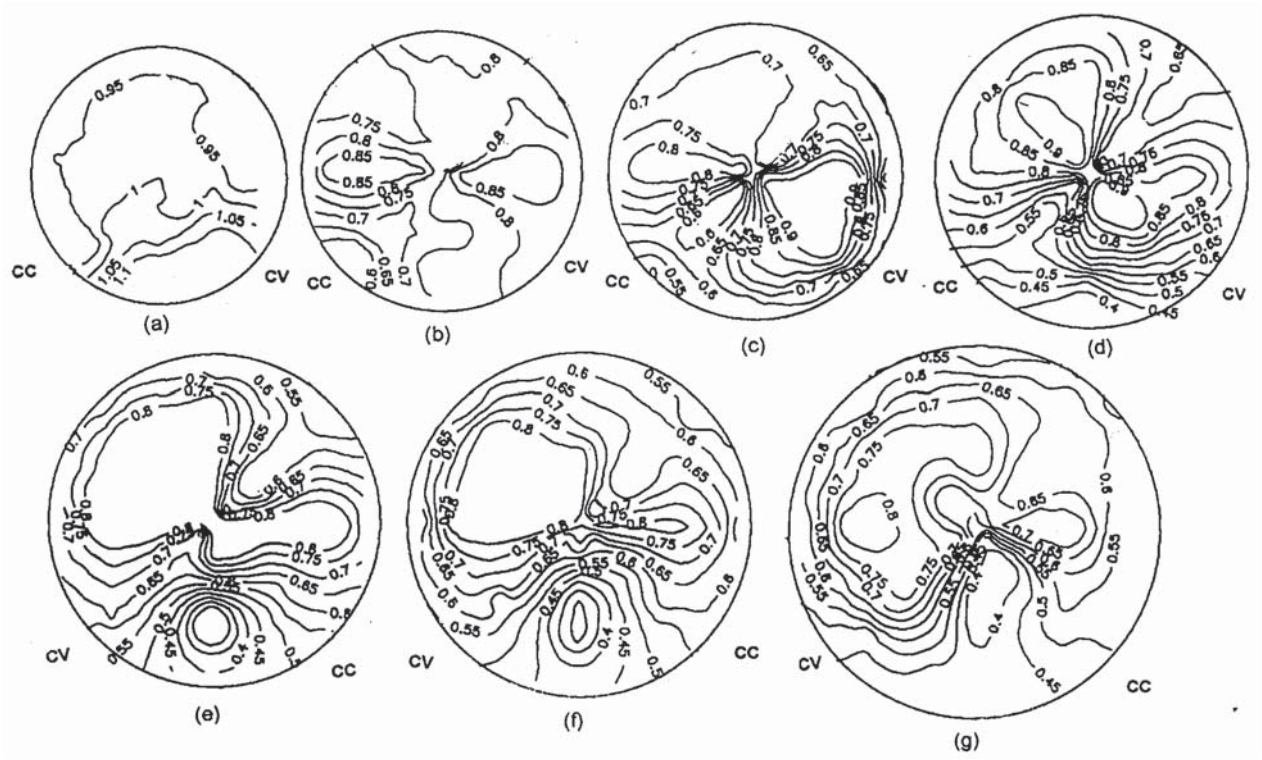

Fig. 6 Constant mean velocity contours at different sections along the length of the diffuser

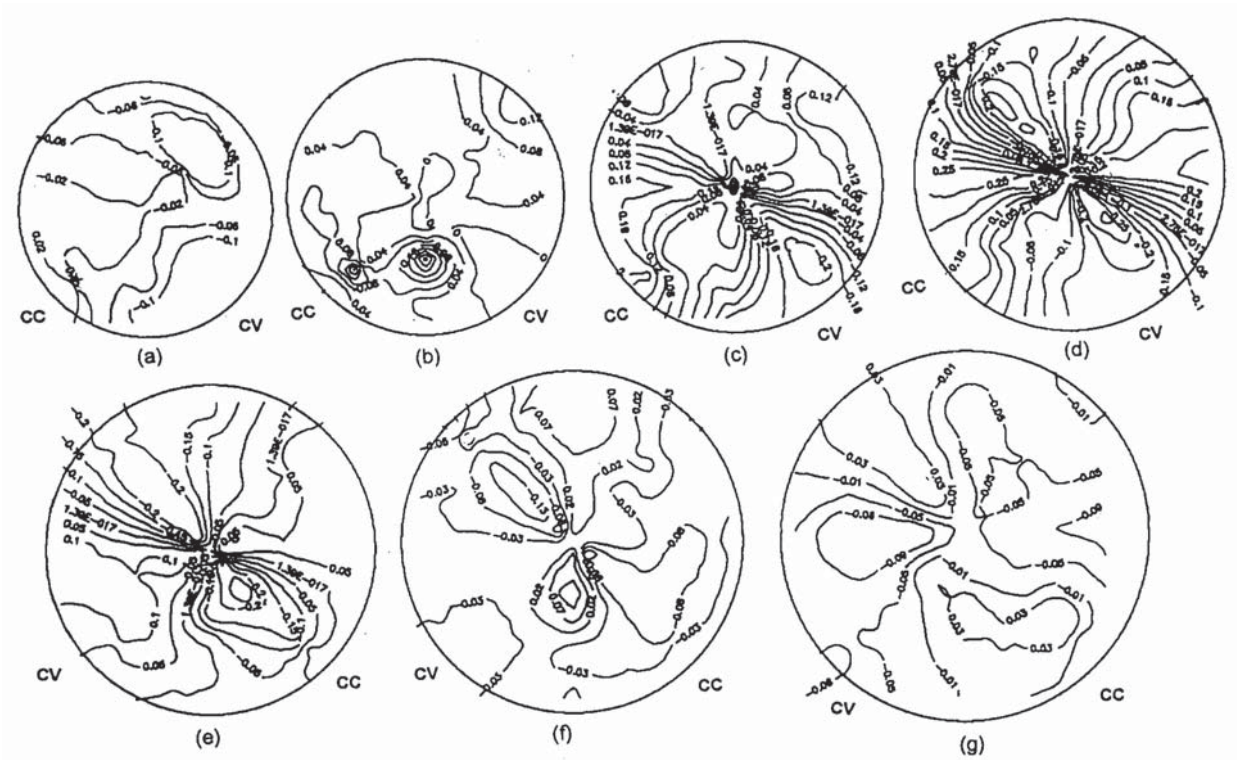

Fig. 7 Constant radial velocity contours at different sections along the length of the diffuser

Figure 7 represents the normalized radial velocity contours along the length of the diffuser. It shows the development of small secondary motion at inlet and its attenuation in the first bend and its movement from one wall to other as already discussed. Change of flow rotation of the secondary motion also been observed in the second bend compared to the previous half and strength of the counter rotating vortices increases in the downstream sections of the diffuser. These observations are in line with Taylor et al. [4], Whitelaw et al. [7], Yu [16].

Figure 8 shows the variation of average normalized mean velocity and average radial velocity along the axis of the diffuser. The average normalized mean velocity decreases continuously in the downstream direction up to 30% of the centerline length of the diffuser, which is about +15º turn of the first bend, while the average normalized mean radial velocity increases 50% of the centerline length and then decreases slightly in the second bend.

Normalized wall static pressure distribution along the four mutually perpendicular walls is shown in Fig.9. It indicates an initial decrease in wall static pressure along inside-outside (cvcc) and outside-inside (cccv) walls. This is due to the acceleration of flow within the straight portion of the diffuser. However, the pressure gradients along different regions of the walls are consistent with the observation made in relation to the measurements of mean velocity and radial velocity. The average pressure recoveries along the four mutually perpendicular walls are 52%.

Mass averaged static pressure recovery (C_{PR}) and total pressure loss coefficient (ξ) along the centerline of the diffuser is shown in Fig.10. These were evaluated from the static pressure and total pressure obtained by 5-hole probe at different measuring sections of the diffuser. It has been observed that average pressure recovery increases continuously up to 9º turn of the first bend and there is a slight decrease of C_{PR} between +9º turn of first bend and -9º turn of the second bend, which is mainly due to the pressure loss caused by the change in curvature. Beyond -9º the pressure recovery increases and a maximum pressure recovery $0.2\rho\, U_{avi}^2$ has achieved. The pressure recovery curve is similar to the distribution seen by Rojas et al. [5]. They obtained a C_{PR} value of $0.19\rho\, U_{avi}^2$ for $A_r = 1.5$ for S-shaped diffuser.

The pressure loss coefficient increases continuously to a value of approximately 7% up to +15º turn of the first bend and maximum value of approximately 9% has been

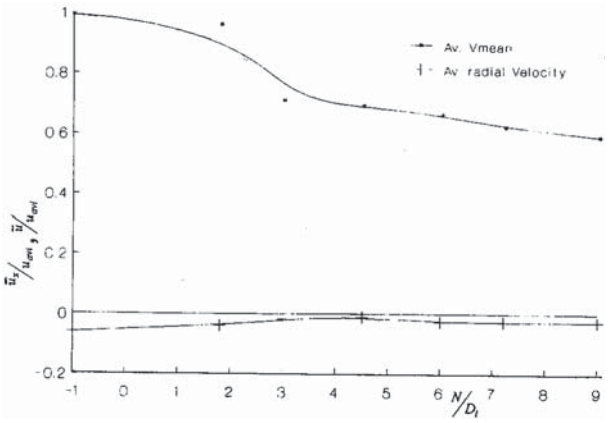

Fig. 8 Variation of average mean velocity and average radial velocity along the length of the diffuser

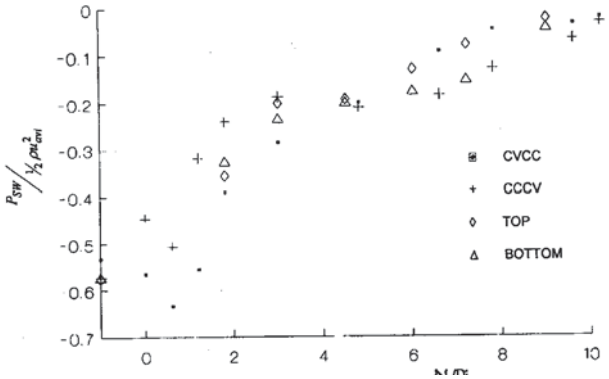

Fig. 9 Wall static pressure variation along the length of the diffuser

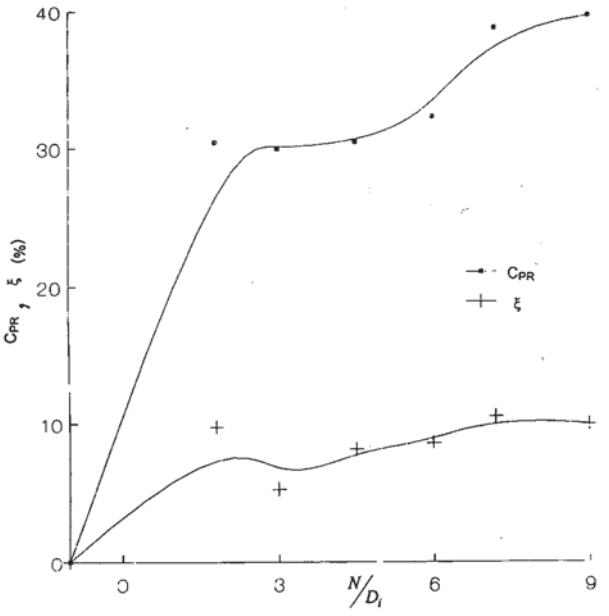

Fig. 10 Variation of mass averaged pressure recovery and loss co-efficient along the length of the diffuser

achieved after -9° turn of the second bend which is equivalent to $0.045\rho U_{avi}^2$. This loss is mainly due to the generation of vortical motion within the diffuser.

Conclusions

The following conclusions can be drawn from the present investigation on an S-shaped diffusing duct.

1. The secondary motion in the form of counter rotating vortices developed due to the imbalance of centrifugal force and radial pressure gradient and changes their sense of rotation in the second half of the bend.
2. The wall pressure along the plane of the curvature increases continuously along downstream with a relatively higher rate of increase along outside-inside (cccv) in the first bend and along inside-outside (cvcc) in the second bend as compared to that in other region. The variation along top and bottom faces is more or less similar to each other.
3. The movement of the core flow behavior is similar to that observed in rectangular S-shaped and constant area S-shaped ducts. It moves in an almost straight path.
4. Mass averaged static pressure recovery is approximately 40% while total pressure loss coefficient is about 9%.

References

1. Rowe, M., "Measurements and Computation of Flow in Pipe Bends", Journal of Fluid Mechanics, Vol.43, Part 4, 1970, pp.771-783.
2. Bansod, P. and Bradsaw, P., "The Flow in S-shaped Ducts", Aeronautical Quarterly, Vol.23, Part 2,1972, pp.131-140.
3. Butz, L. A., "Turbulent Flow in S-shaped Ducts", M.S. Thesis, 1979, Prudue University, U. S. A.
4. Taylor, A. M. K. P., Whitelaw, J. H. and Yianneskis, M., "Developing Flow in S-shaped Ducts, Part II - Circular Cross-section", NASA Contract Report 3759, 1984.
5. Rojas, J., Whitelaw, J. H. and Yianneskis, M., "Developing Flow in S-shaped Diffuser, Part II - Circular Cross-section Diffuser, NASA Contract Report FS/83/28, 1983.
6. Guo, R. W. and Seddon, J., "Swirl Characteristics of an S-shaped Air Intake With Both Horizontal and Vertical Offsets" Aeronautical Quarterly, 1984, pp. 117-127.
7. Whitelaw, J. H. and Yu, S. C. M., "Turbulent Flow Characteristics in an S-shaped Diffusing Duct", Flow Measurement and Instrumentation, Vol. 4, No.3, 1993, pp.171-179.
8. Shimuzu, Y., Nagafusa, M., Sugino, K. and Kubota, T., "Studies on Performance and Internal Flow of U-shaped and Snake-shaped Bend Diffuser", Second Report, ASME, Journal of Fluid Engineering, Vol.108, 1986, pp. 297- 303.
9. Majumder, B., Singh, S. N. and Agrawal, D. P., "Flow Characteristics in S-shaped Diffusing Duct", International Journal of Turbo and Jet Engines, Vol.14, 1997, pp. 45-57.
10. Sullery, R. K., Chandra, B. and Murlidhar., "Performance Comparison of Straight and Curved Diffuser", Defence Scientific Journal, Vol.33, No.3, 1983, pp.195-203.
11. Sonoda, T., Arima, T. and Oana, M., "The Influence of Downstream Passage on the Flow within an Annular S-shaped Duct", ASME, Journal of Turbomachinery, Vol.120, 1998, pp.714-722.
12. Fox, R. W. and Kline, S. J., "Flow Regimes in Curved Subsonic Diffuser" ASME, Journal of Basic Engineering, 1962, pp. 303-316.
13. McMillan, O. J., "Mean Flow Measurements of the Flow Diffusing Bend", NASA Contract Report 3634, 1982.
14. Mullick, A. N., "Turbulent Flow Investigation in an S-shaped Diffusing Duct" M. E. Thesis, Jadavpur University, India, 2000.
15. Kline, S. J., "The Purpose of Uncertainty Analysis" ASME, Journal of Fluid Engineering, Vol. 107, 1985, pp.153-160.
16. Yu, S. C. M., "Turbulent Flow Calculation in S-shaped Diffusing Ducts using a Viscous Marching Technique",VIth International Conference on Computational Methods and Experimental Measurements, 1993, Vol.1, Heat and Fluid Flow.